pdf planosporicin

11 AUTHORS, INCLUDING:

Ameriga Lazzarini
Università degli Studi di Milano-Bicocca

22 PUBLICATIONS **770** CITATIONS

Lucia Carrano
FIIRV - Fondazione Istituto Insubrico di Ricer…

38 PUBLICATIONS **449** CITATIONS

Flavia Marinelli
Università degli Studi dell'Insubria

80 PUBLICATIONS **1,299** CITATIONS

A Novel Lantibiotic Acting on Bacterial Cell Wall Synthesis Produced by the Uncommon Actinomycete *Planomonospora* sp.

Franca Castiglione,[‡] Linda Cavaletti,[‡] Daniele Losi,[‡] Ameriga Lazzarini,[‡] Lucia Carrano,[‡] Marina Feroggio,[‡] Ismaela Ciciliato,[‡] Emiliana Corti,[‡] Gianpaolo Candiani,[‡] Flavia Marinelli,*[,‡,§] and Enrico Selva[§]

Vicuron Pharmaceuticals, Via R. Lepetit 34, 21040 Gerenzano, (VA) Italy, and DBSM, University of Insubria, Via J.H. Dunant 3, 21100 Varese, Italy

ABSTRACT: Important classes of antibiotics acting on bacterial cell wall biosynthesis, such as β-lactams and glycopeptides, are used extensively in therapy and are now faced with a challenge because of the progressive spread of resistant pathogens. A discovery program was devised to target novel peptidoglycan biosynthesis inhibitors capable of overcoming these resistance mechanisms. The microbial products were first screened according to their differential activity against *Staphylococcus aureus* and its L-form. Then, activities insensitive to the addition of a β-lactamase cocktail or D-alanyl-D-alanine affinity resin were selected. Thirty-five lantibiotics were identified from a library of broth extracts produced by 40,000 uncommon actinomycetes. Five of them showed structural characteristics that did not match with any known microbial metabolite. In this study, we report on the production, structure determination, and biological activity of one of these novel lantibiotics, namely, planosporicin, which is produced by the uncommon actinomycete *Planomonospora* sp. Planosporicin is a 2194 Da polypeptide originating from 24 proteinogenic amino acids. It contains lanthionine and methyllanthionine amino acids generating five intramolecular thioether bridges. Planosporicin selectively blocks peptidoglycan biosynthesis and causes accumulation of UDP-linked peptidoglycan precursors in growing bacterial cells. On the basis of its mode of action and globular structure, planosporicin can be assigned to the mersacidin (20 amino acids, 1825 Da) and the actagardine (19 amino acids, 1890 Da) subgroup of type B lantibiotics. Considering its spectrum of activity against Gram-positive pathogens of medical importance, including multi-resistant clinical isolates, and its efficacy *in vivo*, planosporicin represents a potentially new antibiotic to treat emerging pathogens.

Multi-resistant Gram-positive pathogens are increasingly emerging, making it difficult to treat infections effectively with antibiotics. A survey of this problem indicates that in the United States ca. 25% of *Streptococcus pneumoniae* are resistant to penicillin, ca. 35% of *Staphylococcus aureus* are resistant to all available β-lactam antibiotics, and ca. 12% of *Enterococcus faecalis* are resistant to vancomycin (*1*). Recently, highly vancomycin-resistant *Staphylococcus aureus* (VRSA) isolates have appeared in clinical specimens (*2*). This is a matter of concern because the glycopeptides vancomycin and teicoplanin (the latter registered in Europe) have been extensively used as drugs of last resort against multi-resistant staphylococci. Novel antibiotics with unexploited mechanisms of action are thus desirable as they are likely capable of overcoming existing resistance mechanisms.

A generalized discovery approach involves target-based screening using an assay based on bacterial vital targets. One such validated target is bacterial cell wall biosynthesis. This pathway is restricted to prokaryotes and thus predictive of low intrinsic toxicity to mammals. It also features remarkable structural and functional complexity and may thus be

impaired by inhibiting a variety of steps, ranging from the biogenesis of dedicated monomers to specialized assembly, membrane translocation and extracellular cross-linking, and strengthening of the exoskeletal peptidoglycan (PG[1]) (*3*). Several components and individual steps in the cell wall pathway represent still unexploited antibiotic targets, which offers an opportunity to discover novel inhibitors that are likely capable of bypassing the resistance mechanisms currently prevalent.

β-Lactam and glycopeptide antibiotics, such as thienamycin (*4*) and vancomycin (*5*), are PG synthesis inhibitors

---

* To whom correspondence should be addressed. Tel: +39 0332 421546. Fax: +39 0332 421500. E-mail: flavia.marinelli@uninsubria.it.
‡ Vicuron Pharmaceuticals.
§ University of Insubria.

[1] Abbreviations: D-Ala-D-Ala, D-alanyl-D-alanine; Dha, dehydroalanine; Dhb, dehydrobutyrine; DMSO, dimethyl sulfoxide; DQF-COSY, double-quantum filtered correlation spectroscopy; ED$_{50}$, antibiotic dose at 50% of *in vivo* efficacy; ESI-MS, electrospray ionization mass spectrometry; HMBC, heteronuclear multiple bond correlation; HMQC, heteronuclear multi-quantum correlation; HPLC, high performance liquid chromatography; LC-MS, liquid chromatography coupled to mass spectrometry; IC$_{50}$, inhibitor concentration at 50% of inhibition; Lan, lanthionine; Melan, 3-methyllanthionine; MIC, minimal inhibitory concentration; MS, mass spectrometry; MS/MS, tandem mass spectrometry; NMR, nuclear magnetic resonance; NOESY, nuclear Overhauser enhancement spectroscopy; PDA, photo diode array detector; PEP, phosphoenolpyruvate; PG, peptidoglycan; TCA, trichloroacetic acid; TFA, trifluoroacetic acid; TOCSY, total correlation spectroscopy; UDP-MurNAc-pentapeptide, uridinediphospho-*N*-acetylmuramyl-L-Ala-D-Glu-L-Lys-D-Ala-D-Ala; UMP, uridine monophosphate.

produced by actinomycetes. This class of microorganisms was screened at Lepetit, the parent group of Vicuron Pharmaceuticals, and led to the discovery of the glycopeptides teicoplanin (6) and A40926 (7), the precursor of dalbavancin (8), and the lipodepsipeptide ramoplanin (9), which have been developed for medical use. We devised a strategy for identifying cell wall inhibitors different from β-lactams and glycopeptides by screening the Vicuron library of 120,000 broth extracts obtained by fermenting 40,000 actinomycetes isolated in the environment. Most of the screened actinomycetes belonged to uncommon genera, that is, they were difficult to isolate and/or cultivate and thus potentially yet unexploited for industrial research (10). Using this approach, five novel lantibiotics were identified.

Lantibiotics are ribosomally synthesized and post-translationally modified peptides produced by Gram-positive bacteria (11). They contain thioether intramolecular cross-linked amino acids termed lanthionines (Lans) or methyllanthionines (Melans) in addition to the unsaturated amino acids 2,3-didehydroalanine (Dha) and (Z)-2,3-didehydrobutyrine (Dhb) (12−14). On the basis of their structural and functional features, lantibiotics are currently divided into two groups. The flexible amphiphilic type A lantibiotics act primarily by forming pores in the bacterial membrane, a mechanism that was shown to involve interaction with lipid II as the docking molecule (15). Their prototype is nisin, which has been used in the dairy industry for over 40 years (11). The type B lantibiotics are more rigid and globular molecules, which inhibit enzyme functions through interaction with the respective substrates: mersacidin (16) and actagardine (also termed gardimycin) (17, 18) inhibit cell wall biosynthesis by forming a complex with lipid II (19), whereas cinnamycin-like peptides inhibit phospholipases by binding phosphatydilethanolamine (20). The present paper deals with the discovery and the initial profiling of Planosporicin, whose structure is substantially different from other known lantibiotics. According to its structural and functional features, planosporicin has been assigned to the actagardine-mersacidin subgroup of type B lantibiotics.

EXPERIMENTAL PROCEDURES

Bacterial Strains. Bacillus megaterium ATCC 13632 and *Staphylococcus aureus* 209 ATCC 6538P (L100) were purchased from American Type Culture Collection (ATCC). *Streptococcus pyogenes* C 203 (21) and other clinical isolates were maintained in the Lepetit Culture Collection (L) c/o Vicuron Pharmaceuticals, Gerenzano, Italy. *Planomonospora* sp., the producer of planosporicin (initially patented as Antibiotic ID97518), was previously isolated in our laboratory from a soil sample using a method by which actinomycetes were enriched with motile spores. It was deposited as *Planomonospora* sp. DSM14920 in DSMZ (Deutsche Sammlung von Mikroorganismen und Zellkulturen GmbH, Braunschweig, Germany) (22).

HTS Primary Screening. One hundred-twenty thousand microbial extracts from 40,000 actinomycetes were screened in liquid microplate assays for their antimicrobial activity to *S. aureus* 209 ATCC 6538P (L100) and to its L form cells (L3751), prepared as previously described (17), and maintained at −80 °C in Nutrient Broth (Difco) to which 20% v/v glycerol was added. Enterococcal Brain Heart

Infusion/S (EBH/S) (23) supplemented with 5% horse serum was used as medium. For the wild-type inoculum, 10 μL of extracts previously dissolved in DMSO/H_2O 1:9 (v/v) were added to 1×10^5 CFU mL^{-1} in 90 μL of culture broth. For L-form cells, aliquots of liquid cultures grown overnight in EBHI/S to $A_{620nm} = 0.2$ were used as inoculum. Incubation time was 24 h at 35 °C in air, and then growth inhibition was measured as O.D. at 620 nm. To validate the assay, standard antibiotic solutions (Table 1) were added, and MICs were determined by broth microdilution assay as recommended by the National Committee for Clinical Laboratory Standards (24).

β-Lactamase Secondary Assay. Antimicrobial activity versus *S. aureus* 209 ATCC 6538P (L100) was measured in a liquid microplate assay as described above after adding the following cocktail of β-lactamases: Penicillase Type I from *Bacillus cereus* (Sigma P0389), 0.001 U/mL; Penicillase Type II from *Bacillus cereus* (Sigma P6018), 0.002 U/mL; Penicillase type III from *Enterobacter cloacae* (Sigma P4399), 0.0025 U/mL; and Penicillase type IV from *Enterobacter cloacae* (Sigma P4524), 0.5 U/mL.

D-*Ala*-D-*Ala Secondary Assay.* Antimicrobial activity versus *S. aureus* 209 ATCC 6538P (L100) was measured in a liquid microplate assay as described above after adding 2 mg/mL of ε-amino-caproyl-D-alanyl-D-alanine, a glycopeptide affinity resin prepared as described elsewhere (25).

Antibiotic Effect on the Cytoplasmic PG Precursor Pool. B. megateriunm ATCC 13632 was cultivated in 100 mL Difco Mueller Hinton Broth (MHB) at 37 °C to an $A_{540nm} = 0.7$. The culture was then divided into equal portions supplemented with antibiotic concentrations that were 100-fold greater than the MICs against *B. megaterium.* Vancomycin, teicoplanin, planosporicin, and chloramphenicol were added at concentrations of 20, 20, 100, and 100 μg/mL, respectively. The cytoplasmic PG precursor pool was analyzed according to ref 26. Briefly, after a 60 min incubation period at 37 °C, the cells were harvested, suspended in water (0.1 g fresh weight per mL), and boiled for 20 min. After cooling first at room temperature and then in ice, the suspension was centrifuged at 39,000g for 30 min. The supernatant was lyophilized and dissolved in 0.1 volumes of water adjusted to pH 3 with formic acid. The samples were analyzed by reversed-phase HPLC and ESI-MS as described below.

Inhibition of Macromolecular Synthesis. S. aureus 209 ATCC 6538P (L100) was cultivated in Iso-Sensitest Broth (ISS, Oxoid Ltd.) overnight at 37 °C. The culture was then diluted 1:1 (v/v) in Davis Mingioli Broth/ISS. At $A_{540nm} = 0.4$, macromolecular syntheses (DNA, RNA, protein, and cell wall PG) were monitored by incorporating the appropriate radioactive precursors: for DNA synthesis, [³H]-thy (5 μCi/mL) with 0.1 g/L unlabeled adenosine; for RNA synthesis, [5,6-³H]-Ura (2μCi/mL); for protein synthesis, L-[³H]-leucine (10 μCi/mL); and for cell wall PG, *N*-acetyl-D-[1-³H] glucosamine (1 μCi/mL) with 3.5 mg/L unlabeled *N*-acetylglucosamine. Of the resulting solutions, 100 μL were dispensed in 96-well microplates containing 10 μL of increasing concentrations of planosporicin, teicoplanin, actagardine, or nisin. After 20 min of incubation at 37 °C, 0.1 mL of ice-cold 20% (w/v) TCA was added to precipitate macromolecules. After 30 min at 4 °C, the TCA precipitate

Table 1: Effect of Known Antibiotics on *S. aureu*s ATCC 6538P and on Its L-form Cells[a]

inhibitor	antibiotic class	target	*S. aureus* wild type MIC (μg/mL)	*S. aureus* L-form	MIC L-form/ MIC wild type
ACTAGARDINE	lantibiotic	cell wall	32	>256	>8
TEICOPLANIN	glycopeptide	cell wall	0.5	>128	>256
VANCOMYCIN	glycopeptide	cell wall	0.25	>512	>1024
RAMOPLANIN	lipodepsipeptide	cell wall	0.13	32	246
ENDURACIDIN	lipoglycopeptide	cell wall	0.13	>128	>984
PENICILLIN G	penicillin	cell wall	0.13	>128	>984
OXACILLIN	penicillin	cell wall	0.13	>128	>984
AMPICILLIN	penicillin	cell wall	1	>128	>128
METHICILLIN	penicillin	cell wall	0.5	>128	>256
CEFUROXIME	cephalosporin	cell wall	0.5	>128	>256
CEFOXITIN	cephalosporin	cell wall	4	>128	>32
CEFAZOLIN	cephalosporin	cell wall	0.25	>128	>512
IMIPENEM	carbapenem	cell wall	0.13	>128	>984
FOSFOMYCIN	pep derivative	cell wall	1	>500	>500
D-CYCLOSERINE	aminoacid derivative	cell wall	16	>500	>31.25
BACITRACIN	peptide	cell wall[b]	32	128	4
NISIN	lantibiotic	membrane[c]	0.5	16	32
ERYTHROMYCIN	macrolide	protein synthesis	0.13	0.06	0.461
STREPTOMYCIN	aminoglycoside	protein synthesis	32	8	0.25
KANAMYCIN	aminoglycoside	protein synthesis	8	4	0.5
GENTAMICIN	aminoglycoside	protein synthesis	2	1	0.5
NEOMICIN	aminoglycoside	protein synthesis	4	2	0.5
CHLORAMPHENICOL	chorismate-derivative	protein synthesis	2	1	0.5
NALIDIXIC ACID	quinolone	DNA replication	32	32	1
CIPROFLOXACIN	quinolone	DNA replication	0.5	0.25	0.5
NOVOBIOCIN	coumarin glycoside	DNA replication	0.06	0.06	1
RIFAMPIN	ansamycin	RNA polymerase	0.004	0.001	0.25
GE2270	thiopeptide	protein synthesis	0.06	0.03	0.5

[a] Serial dilutions of each antibiotic were added to the liquid microtiter assay as described in Experimental Procedures. MICs were determined by the microbroth dilution method (*24*). [b] Membrane compartment (*3*). [c] Mediated by binding to lipid II (*15*).

was collected on glass fiber filters (Filtermat A, Wallac) using a 96-well cell harvester (Wallac), and radioactivity was determined in a β-plate scintillation counter (Wallac).

MIC Determinations. In vitro antimicrobial activity was determined by a broth microdilution assay as recommended by the National Committee for Clinical Laboratory Standards (*24*). The growth media utilized to determine the MIC were: cation adjusted Difco Mueller Hinton Broth (MHB) for staphylococci, enterococci, bacilli, *Moraxella catarrhalis*, and *Escherichia coli*; Todd Hewitt Broth (THB) for streptococci; Lactobacilli MRS broth (MRS) for lactobacilli; Wilkins Chalgren broth for *Clostridium*; and RPMI-1640 medium (RPMI) for *Candida albicans*. Typically, a 2-fold serial dilution of the test compound was performed in a sterile 96-well microplate inoculated with 10^4 CFU/mL of the test strain in the appropriate medium. The microplate was then incubated for 18−24 h at 35 °C. The MIC was determined by visual examination of the microplates with the aid of a magnifying mirror as the lowest concentration of antibiotic that showed no visible sign of microbial growth.

Experimental Septicemia. Female outbred ICR(CD-1) mice (Harlan Italia) weighing 14−16 g were infected intraperitoneally (ip) with 6.5×10^2 cells of *S. pyogenes* C 203 (*21*) in 0.5 mL of saline supplemented with 1% peptone. Planosporicin was administered intravenously (iv) or subcutaneously (sc) within 10−15 min after infection. Teicoplanin was used as the reference drug and was administered sc. The 50% effective dose (ED_{50}) was calculated by the Spearman−Kärber method (*27*) from the percentage of animals surviving to the seventh day at each dose.

Fermentation. Planomonospora sp. DSM14920 was cultivated at 28 °C and shaking at 200 rpm in 500 mL Erlenmeyer flasks containing 100 mL of seed medium AF/ MS (in g/L: dextrose 20, yeast extract 2, soybean meal 8, NaCl 1, and $CaCO_3$ 4, pH adjusted to 7.3) or in Chemap-Braun 20 L fermenters containing 15 L of the same medium at 28 °C and stirring at 600 rpm and 0.5 vvm aeration. For fermentation, 300-L Bioengineering fermenters were used, which contained 200 L of the production medium M8 (in g /L: starch 20, glucose 10, yeast extract 2, hydrolyzed casein 4, meat extract 2, and $CaCO_3$ 3, pH adjusted to 7.0) inoculated with 7% of pre-culture, at 28−30 °C, stirred at 180 rpm, and aerated at 0.5 vvm. The production of planosporicin was monitored by HPLC as described below. Growth was measured as packed mycelium volume (PMV%) by centrifuging 10 mL of culture in graduated vials.

Isolation and Purification of Planosporicin. Broth was harvested after 260 h of fermentation, brought to pH 3 with concentrated sulfuric acid, and then filtered. The filtrate was stirred with 2.6% (v/v) HP 20 polystyrene resin (Mitsubishi Chemical Co.). The resin was then recovered, washed batchwise with methanol/water 1:1 (v/v), and eluted with methanol/ *n*-butanol/water 9:1:1 (v/v/v). The fractions containing the antibiotic were pooled and concentrated under vacuum. Crude antibiotic was precipitated upon addition of acetone. The precipitate was purified on a Lichrosorb RP8 (Merck, Darmstad) 25 × 250 mm column (7 μm particle size), which was eluted at a 30 mL/min flow rate with the following sequence of linear gradients of CH_3CN in 20 mM ammonium formate buffer at pH 4.5: from 10% to 25% in 10 min, from 25% to 40% in 32 min, and from 30% to 90% in 5 min.

Detection was at 230 nm. Planosporicin typically eluted after 26 min under these conditions.

HPLC Analysis. The fermentation and purification processes were monitored by HPLC on a Shimadzu instrument equipped with an Ultrasphere 250 × 4.6 mm column (Beckman Instruments Inc.), 5 μm particle size, and eluted at a 1 mL/min flow rate with a linear gradient from 10% to 90% phase B (20 mM ammonium formate pH 4.5 buffer: CH$_3$CN 5:95 v/v), in phase A (20 mM ammonium formate pH 4.5 buffer: CH$_3$CN 95:5 v/v) for 28 min. Detection was at 230 nm. Planosporicin typically eluted after 23.7 min under these conditions.

LC-MS and MS/MS Analyses. LC-MS and MS/MS experiments were performed using a ThermoQuest Finnigan LCQ Deca mass detector equipped with an ESI interface and a Thermo Finnigan Surveyor MS pump, PDA detector (UV6000, Thermo Finnigan), and an autosampler, as described elsewhere (*28*). The MS spectra were obtained by electrospray ionization both in positive and negative mode under the following conditions. (1) Sample inlet conditions: capillary temperature 250 °C; sheat gas (N$_2$), 80 LCQ arbitrary units; auxiliary gas (N$_2$), 20 LCQ arbitrary units; (2) Sample inlet voltage settings: positive polarity, 4.5 kV; negative polarity, 2.8 kV; capillary voltage, 4 V; and tube lens offset, 30 V. Helium was used as the buffer and collision gas. MS/MS analyses were performed at collision energy levels ranging from 25 to 50 kV. All of the spectra were acquired in the 150−2000 mass unit range, unless otherwise stated.

Microbial extracts were separated on a Waters Symmetry shield RP18, 250 × 4.6 mm column (Waters Chromathography), and 5 μm particle size, eluted at a 1 mL/min flow rate, with a linear gradient from 10% to 90% of phase B (CH$_3$CN) in phase A (20 mM ammonium formate pH 4.5 buffer: CH$_3$CN 5:95 v/v) for 28 min. Detection was at 230 nm. The effluent from the column was split in a ratio of 95:5 between PDA and MS detector. Bioautographies of the HPLC fractions were performed with test organisms in a liquid microplate assay as described above.

Cytoplasmic PG precursors were separated on a C18 250 × 4.6 mm column (Phenomenex Luna), 5 μm particle size, eluted at a 1 mL/min flow rate with a 2 min 100% phase A (2% CH$_3$CN/97.9% H$_2$O/0.1% HCOOH v/v/v) and then a 50 min linear gradient to 100% phase B (95% CH$_3$-CN/4.915% H$_2$O/0.085% HCOOH v/v/v). Column temperature was 22 °C. The effluent from the column was split in a ratio of 1:5 between the PDA and MS detector.

In the infusion experiments, planosporicin was diluted to 0.01 mg/mL (5.5 pmol/μL) in H$_2$O/CH$_3$CN 50:50 v/v. The ThermoQuest Finnigan LCQ Deca mass detector was previously tuned and calibrated in electrospray mode using Ultramark 1621 (Thermo Finnigan), caffeine, and L-ethionylarginyl-phenylalanyl-arginine (Sigma-Aldrich) in infusion mode at 5 μL/min.

Hydrolysis and Amino Acid Analysis. Planosporicin (1 mg) was completely hydrolyzed by treatment for 24 h in 6 N HCl at 105 °C. The mixture of hydrolyzed amino acids was treated with *N*-hydroxysuccinimide-activated heterocyclic carbamate Waters AccQ-Fluor Reagent Kit (*29*) and was then analyzed by LC-MS. The separation procedure was performed at 37 °C on a C18 AccQ-TagTM Waters column (3.9 × 150 mm) eluted at a 1 mL/min flow rate with the following multistep gradient: 5 min with 5% phase B, then

a 30 min linear gradient to 80% phase B, followed by 10 min with 95% phase B. Phase A comprised 140 mM ammonium acetate, pH 5 buffer, and phase B H$_2$O/CH$_3$CN 60:40 (v/v). The effluent from the column was split between the PDA and MS detectors. The MS parameters were the same as those described above, and the spectra were acquired in the 100−700 mass unit range.

NMR Spectroscopy. NMR spectroscopic analyses were performed on two planosporicin samples of 5 mg (for 1D and 2D proton spectra) or 12 mg (for 1D carbon and 2D heterocorrelated spectra) in 0.6 mL H$_2$O/D$_2$O 9:1 (v/v) adjusted to pH 2.3−2.4 with TFA and supplemented with drops of acetonitrile to solubilize the antibiotic. The H 1D spectrum (using watergate presaturation sequence), two-dimensional DQF-COSY, TOCSY, and NOESY experiments were performed at 293 and 313 K using a Bruker DRX 750 MHz spectrometer. In all of the experiments, 2D spectra were recorded with a spectral width of 14 ppm, 48 scans, 1024 increments in t$_1$, and 4096 complex data points in t$_2$. For the TOCSY experiments we used a 70 ms clean MLEV17 spin lock for isotropic mixing, whereas NOESY spectra were acquired with 80, 180, and 300 ms mixing times. Natural abundance heteronuclear ^{13}C-{^{1}H} HSQC and HMBC experiments were performed at 313 K. For the ^{13}C-{^{1}H} 1D spectrum, a sweep width of 220 ppm was used; 40 K scans were obtained with a relaxation delay of 2 s. The HSQC and HMBC spectra were acquired at 1024 t$_1$ increments and 2048 complex data points in t$_2$, using a sweep width of 14 ppm in the proton and 199 ppm in the carbon dimension. A series of ^{15}N-{^{1}H} HSQC spectra were recorded on the more concentrated sample of planosporicin at different temperatures, ranging from 283 to 313 K in steps of 10 K. All of these experiments were performed on a Bruker Advance 600 MHz spectrometer equipped with a 5 mm cryoprobe system.

RESULTS

Screening of Microbial Products. Primary screening of the 120,000 microbial extracts from the Vicuron library was based on the differential activity assay versus *S. aureus* and its L-form. L-forms are protoplast-type cells derived from *S. aureus* that are able to replicate in appropriate osmotic conditions despite the lack of a functional cell wall (*17*). As shown in Table 1, L-forms are equally or more sensitive than parental cells to antibiotics acting on molecular targets other than cell wall biosynthesis. They are indeed resistant to PG synthesis inhibitors. The MICs for reference β-lactams and glycopeptides, and other known cell wall inhibitors, versus L-form cells, were at least 8-fold higher than those against the whole cells. This level of differential activity was found in 3% of the screened microbial extracts. Secondary selection was based on whether antimicrobial activity against *S.aureus* could be reversed by a β-lactamase cocktail or by adding D-Ala-D-Ala affinity resin (*25*). The majority of the extracts selected during the primary screening were therefore discarded because their activity was due to β-lactams susceptible to β-lactamases or to D-Ala- D-Ala binding glycopeptides. Other extracts were also discarded because of the lack of novelty after LC-MS analysis or because they did not yield consistent results upon repeated fermentation of the producing strains. Lantibiotic molecules were highlighted in 35 broth extracts according to their LC-MS profiles coupled with
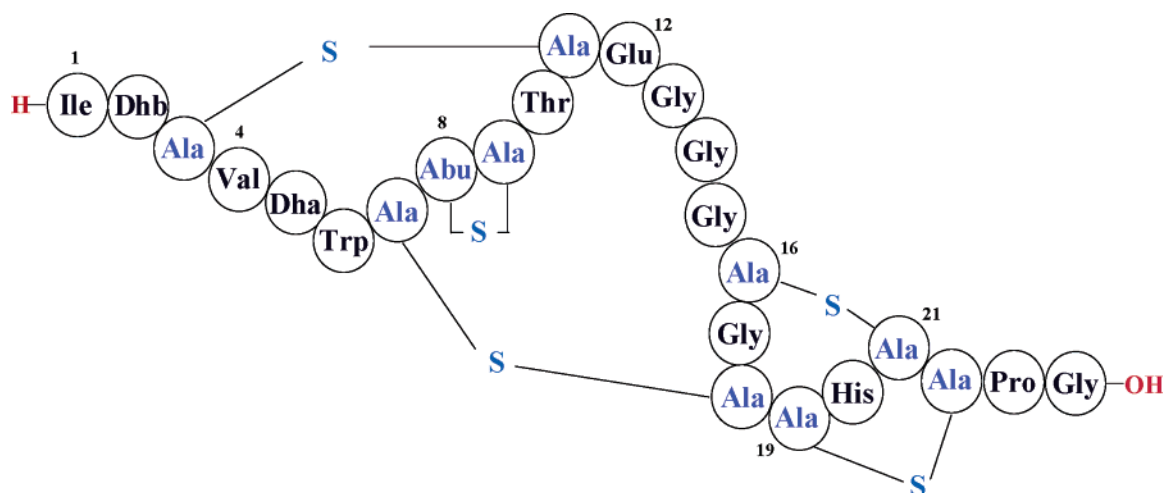
FIGURE 1: Primary structure of the antibiotic planosporicin.

bioautography and by searching for the characteristic Lan and Melan amino acids in the acid hydrolysates of the crude extracts. Actagardine (*17, 18*) was recurrently identified. Besides actagardine, five distinct lantibiotics, whose chemical properties did not match with any known microbial metabolite, were isolated. In this article, we describe the structure and the initial biological profiling of the lantibiotic called planosporicin (previously patented as ID 97518), produced by an uncommon actinomycete, *Planomonospora* sp. DSM14920 (*22*).

Production and Purification of Planosporicin. Planomonospora sp. DSM14920 grew and produced planosporicin in the fermentation media commonly used for actinomycetes. The production commenced after ca. 48 h from the time of inoculum and reached a maximum (ca. 280 mg/L) after 100−120 h of fermentation (data not shown). Most of the antibiotic (90%) was secreted into the broth. The pure antibiotic was obtained from the filtered broth by multistep chromatography, as described in Experimental Procedures, and remained stable during the purification process. The stability of planosporicin was checked at different pH values and temperatures. In the pH range from 2 to 6.5, the antibiotic half-life was more than 1 month, decreasing to 10−15 days at pH values from 6.5 to 7.5. No degradation was observed when planosporicin was incubated at temperatures ranging from 288 to 313 K.

Structure Elucidation of Planosporicin. The complete ^{1}H NMR spectrum reflected a pattern typical for small peptide molecules. By analyzing DQF-COSY and TOCSY experiments as described in refs *30* and *31*, we were able to identify and assign the amino acid spin systems; the resulting planosporicin structure is presented in Figure 1. These experiments revealed that eight proteinogenic amino acid spin systems occur only once: Trp, His, Thr, Ile, Val, Ala, Pro, and Glu. The Gly spin system appeared four times. Two aromatic ring systems were assigned by examining the aromatic region of the DQF-COSY spectrum. Some doublets and triplets, corresponding to the Trp and His rings, respectively, were observed. Connectivities between the aromatic ring protons and their backbone protons could only be established through the NOESY experiments because there was no mutual coupling. In addition, spin systems of those amino acids characteristic of lantibiotics were present. Dha and Dhb were found in the characteristic spectral region 5.5−7 ppm (*32*). Finally, the α-aminobutyric acid (Abu) part

of the Melan unit appeared once, and the Ala part of the Lan amino acid gave rise to nine ABMX spin systems. This is consistent with the presence of five rings formed by sulfide bridges in the antibiotic structure. The majority of the amide protons were observed and assigned to the corresponding CHα. Some partial overlapping resonances at 8.04 ppm (later attributed to Ala7, Ala18, and Gly15) could be explained by performing 2D experiments at different temperatures. The proton chemical shifts of the individual amino acids of planosporicin together with their CHα-NH coupling constants are reported in Table 2. To assign the sequence of unlabeled peptides and proteins, a search for short-range NOESY cross-peaks must be performed between the CHα, CHβ, or amide proton of (*i*) residue and the amide proton of the adjacent (*i* + 1) residue in the peptide sequence (*33*) denoted by αN, βN, and NN, respectively. In planosporicin, a sequence of such NOEs could be traced for the majority of the amino acid residues, corresponding to the peptide sequence shown in Figure 1. The 2D NOESY spectrum, reported in Supporting Information, indicates the sequential assignments of constituents that can be associated, in biosynthetic terms, to 24 amino acids. Table A in the Supporting Information reports the complete NOE connectivity matrix. Using the unique single occurrence of the Val, Dha, and Trp residues, the initial NH₂ sequence NH₂-Ile-Dhb-Ala-Val-Dha-Trp was readily established. Using the information from NOESY spectra acquired at 313 and 293 K in a similar manner, together with the HMBC data, it was possible to sequentially assign the rest of the molecule.

The position of the sulfide bridges could be deduced from [13]C-^{1}H multiplebond correlations $\underline{C}-S-C-\underline{H}$ between the two amino acids forming the bridge and then confirmed by NOE cross-peaks between β protons in the L-alanine and the D-alanine fragments of Lan. In the present case, the following connectivities were observed: Ala3-Ala11, Ala7-Ala18, Abu8-Ala9, Ala16-Ala21, and Ala19-Ala22. The ^{13}C resonances were assigned by using the HSQC and HMBC spectra; with the HSQC spectrum, all of the carbons could be assigned without overlap. The carbon chemical shifts of all amino acid residues are listed in Table B in the Supporting Information.

MS analyses were performed on the hydrolyzed and intact antibiotic to further confirm the structure assigned by NMR. The LC-MS analysis of the hydrolysis mixture showed the

Table 2: Proton Chemical Shifts (ppm) of the Individual Amino Acids Constituting Antibiotic Planosporicin Together with Their J(NH−CHα) Coupling Constants (Hz) and Amide Temperature Coefficients (−ppbK^{-1})^a

residue	NH	CHα	CHβ	others	J(NH−CHα)	$\Delta\delta/T$
Ile1		4.01	1.97	CHγ 1.18−1.43 Me 0.86−0.97		
Dhb2	9.71		6.5	Me 1.7		6.5
Ala3	8.07	4.25	2.81−3.2			5.5
Val4	7.87	4.02	2.13	Me 0.79−0.83	7.7	5
Dha5	8.9		5.26−5.75			5.1
Trp6	8.41		3.19−3.29	**5)** 7.06, **6)** 7.13, **2)** 7.17, **7)** 7.39, **4)** 7.58, 9.98	6.6	6.5
Ala7	8.03	4.5	2.98−3.06			4.5
Abu8	8.61	4.92	3.47	Me 1.2	9.3	9.5
Ala9	8.07	3.91	2.93−3.55			4.8
Thr10	8.14	4.2	4.11	Me 1.1	7.1	7
Ala11	8.37	4.5	2.9−3.01		7.1	8.1
Glu12	8.15	4.16	1.9−1.98	CHγ 2.33	4.9	4.7
Gly13	8.49	3.77−3.96			5.5	8.5
Gly14	7.8	3.67−3.86			6	2
Gly15	8.04	3.74−3.92				6.1
Ala16	8.65	4.29	3.02−3.08			8.5
Gly17	8.88	3.8−3.97			4.9	9.5
Ala18	8.04	4.23	2.79−3.18			2.1
Ala19	7.97	4.96	3.0		9.3	2
His20	8.66	4.43	3.3−3.37	**2)** 7.28, **4)** 8.55		
Ala21	8.81	4.61	2.6−3.25		9.3	7.5
Ala22	7.29	3.9	2.8−3.57			1.5
Pro23		4.28	1.81−2.23	CHγ 1.7−1.8 CHδ 3.19−3.36		
Gly24	8.54	3.68−4.13				6

^{a} Planosporicin was dissolved in H_2O/D_2O at 313 K.

presence of the Lan, Melan, Gly, Thr, Pro, Val, Glu, His, and Ile amino acids, whereas the residues Dha, Dhb, and Trp were not found, probably because of their instability under the strong acidic conditions applied for hydrolysis.

The mass spectrum of the intact peptide showed the presence of an intense signal at *m/z* of 1097.5 corresponding to the double charged ion [M + 2H]$^{2+}$ (Figure 2). In the full scan spectrum range 300−3000 mass units, the signal corresponding to the single charged ion [M + H]$^+$ 2195 was also present. A molecular mass of 2194 Da was calculated, which is in agreement with the mass determined from the NMR-derived sequence. The ions corresponding to [M + 2H]$^{2+}$ and [M + H]$^+$ were then selected for MS/MS fragmentation at several collision energy values. Eight major peaks were identified in the MS/MS spectra and were found to be consistent with residues 1−23, 2−24, 4−24, 5−24, 6−24, 3−21, 6−23, and 6−22 (Table 3). As observed for other lantibiotics, little cleavage occurred in the central part of the molecule containing the Lan rings, whereas five fragments corresponding to the cleavage of the first Lan ring and one fragment due to the cleavage of the last thioether bridge could be identified. In summary, the NMR and MS results are both consistent with the structure reported in Figure 1.

Secondary Structure of Planosporicin. By analyzing amide proton temperature coefficients and solvent accessibility, we gained insight into the secondary structure of the antibiotic. Typically, hydrogen bond formation stabilizes the exchangeable backbone amide protons and therefore reduces the exchange rate with the bulk solvent. Such stability can also be achieved when solvent accessibility is reduced as a result of steric constraints. Assessing the temperature dependency of the amide proton chemical shifts represents a simple means

of gaining information about the extent to which hydrogens are bonded or sequestered from the solvent (*34, 35*). A low dependency of the amide chemical shift on temperature in an aqueous environment (temperature coefficients $\Delta\delta/\Delta t$ > −2.5 ppb/K) is usually indicative of the presence of a stable hydrogen bond, whereas solvent-accessible amide protons are more sensitive to temperature change ($\Delta\delta/\Delta t$ < −5 ppb/K). We collected several ^{15}N-^{1}H HSQC spectra of the unlabeled peptide at temperatures ranging from 283 to 313 K at steps of 10 K. These data clearly showed that the amide proton chemical shift of Ala18 amide hardly changed with increasing temperature, whereas Ala16, Gly17 and Abu8 were more strongly affected. Table 2 reports the temperature coefficients. According to the aforementioned criteria, stable amide protons with low solvent accessibility were identified in Ala18, Ala19, Ala22, and Gly14. In addition, the sequential NOEs used to assign the resonances (see Table B in Supporting Information) provided further evidence for regions of regular secondary structure in planosporicin. The continuous stretch of medium-range sequential NN connectivities from residues Val4 to Gly17 suggests that this region may adopt a compact rather than an extended conformation. Further work is needed to determine the overall molecular conformation using distance constraints derived from NOESY experiments.

Mode of Action of Planosporicin. Planosporicin was active against *S. aureus* and inactive to its L-forms that lacked a functional cell wall. The cell-wall synthesis target was confirmed by testing the antibiotic effect to macromolecular syntheses in *S. aureus*. Figure 3A shows that PG biosynthesis was blocked by planosporicin at concentrations that showed only marginal effects on DNA, RNA, and protein syntheses. Planosporicin's mode of action was similar to the inhibition
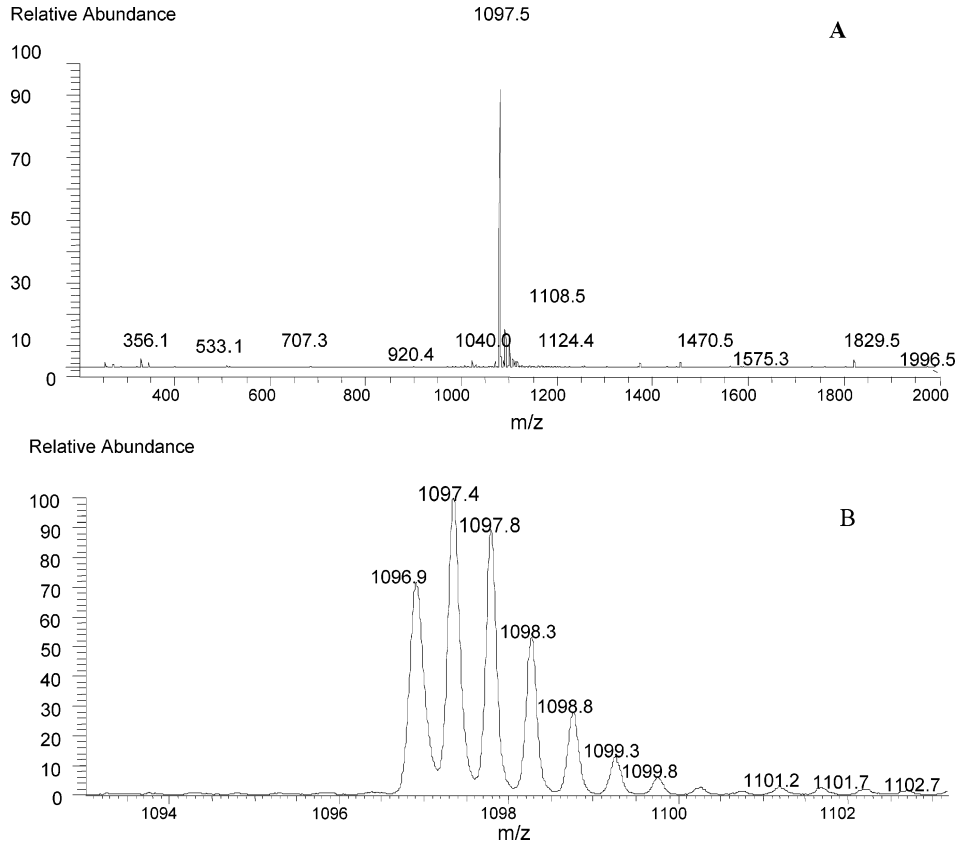
FIGURE 2: Mass spectra of planosporicin obtained from infusion experiments. The signal at 1097.5 corresponds to the [M + 2H]/2 ion. (A) Full-scan low-resolution spectrum. (B) Zoom-scan high-resolution spectrum.

Table 3: Peptide Fragments from MS/MS of the Antibiotic Planosporicin

[M + 2H]/2 (*m/z* ratio)	peptide fragments
1069	fragment 1−23
1013	fragment 2−24
949	fragment 4−24
918	fragment 5−24 (SH)[a]
861	fragment 6−24
847	fragment 3-21 (SH)[a]
831	fragment 6−23
784	fragment 6−22

[a] This fragment contains the SH group.

patterns observed in the glycopeptide teicoplanin (Figure 3B) and the type B lantibiotic actagardine (Figure 3C). Indeed, type A lantibiotic nisin inhibited all four macromolecular syntheses at the same concentration (Figure 3D), consistent with its primary mode of action, by disrupting membrane integrity (*12−15*).

We also examined planosporicin's effect on the cytoplasmatic pool of UDP-linked PG precursors in *B. megaterium*. Upon treatment with planosporicin (Figure 4A), a marked increase in an LC-MS peak was revealed that could not be detected in untreated cells (Figure 4C). An identical peak showing the same MS/MS fragmentation profile was detected when *B. megaterium* cells were treated with vancomycin or teicoplanin (Figure 4B). The corresponding mass spectrum was determined in positive and negative ion mode, as shown in Figure 5A. In Figure 5B, the quasi-molecular ionic area was expanded. The ions at *m/z* 1194.1 and 790.2 were attributed to [M + H]$^+$ and [M − UDP]$^+$, those at *m/z* 1192.2, 595.7, and 403.1 to [M − H]$^-$, [M − 2H]$^-$, and

[UDP]$^-$, respectively, indicating the presence of a compound with a monoisotopic molecular mass of 1193 and containing the UDP moiety. This is consistent with the UDP-MurNAc-L-Ala-D-Glu-*m*Dap-D-Ala-D-Ala structure shown in Figure 5C. Further MS/MS studies, not reported in this article, confirmed the fragmentation indicated in Figure 5C. The fragment ion at *m/z* 1121 corresponded to the loss of the alanine residue and those at *m/z* 868 and 788 to the loss of UMP and UDP, respectively, whereas the ion at *m/z* 403 corresponded to [UDP − H]$^-$.

The accumulation of the cell wall precursor is consistent with the data reported in a variety of bacteria treated with cell wall inhibitors acting at steps subsequent to the synthesis of UPD-MurNAc−pentapeptide in the cytoplasm, such as ramoplanin, vancomycin, teicoplanin, mannopeptimycins (*36, 37*), and type B lantibiotics mersacidin and actagardine (*19, 38*).

Anti-Microbial Activity. Table 4 presents the spectrum of planosporicin's anti-bacterial activity against a panel of important human pathogens. The antibiotic was active against major Gram-positive pathogens, including methicillin-resistant *S. aureus* (MRSA) and vancomycin-resistant enterococci (VRE) (*1, 2*). Planosporicin activity was generally superior to that of actagardine and comparable to that of mersacidin. For purposes of comparison, the MICs for nisin were higher, as expected on the basis of its effect on plasma membrane permeabilization (*12−15*). Lactobacilli were particularly sensitive to planosporicin, including strains reported to be associated with clinical cases of bacteremia or endocarditis (*39*). Planosporicin was more active than mersacidin and actagardine on the anaerobic clostridia.
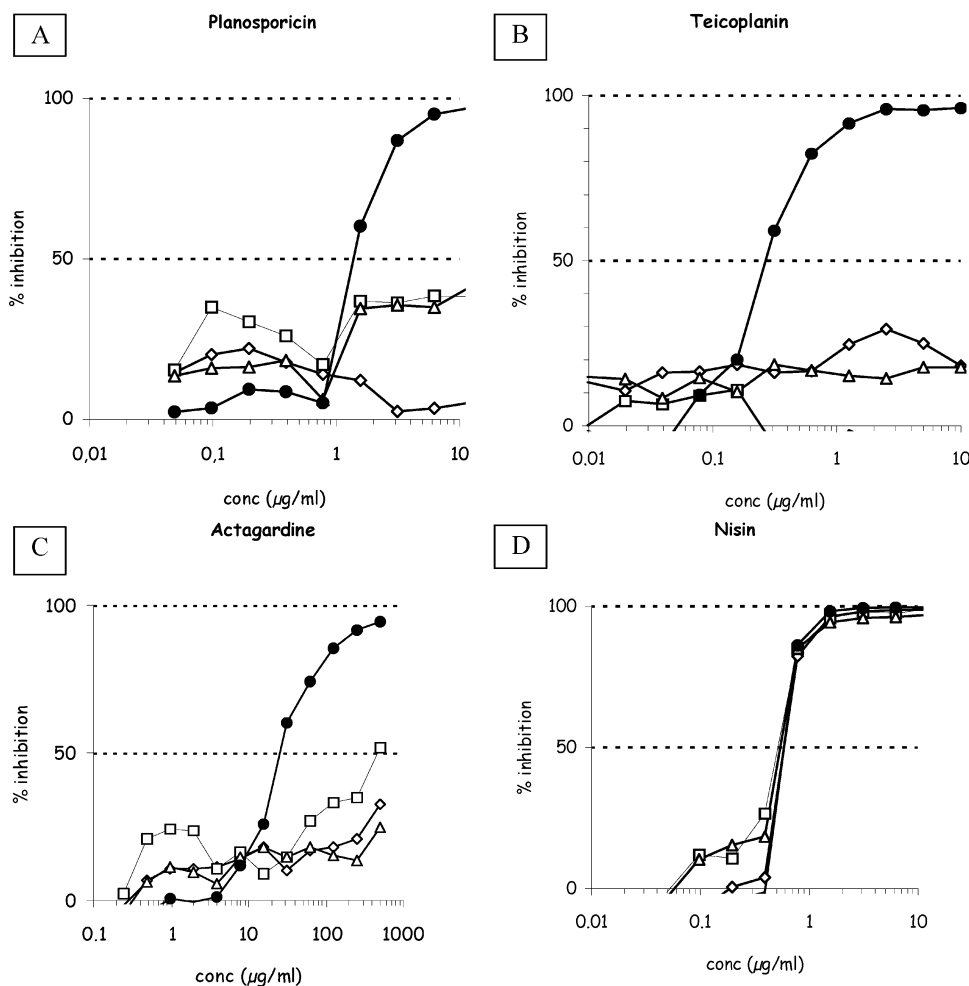
FIGURE 3: Inhibition tests of macromolecular syntheses in *Staphylococcus aureus* by planosporicin (A), teicoplanin (B), actagardine (C), and nisin (D). The effect of the antibiotic on DNA (◇), RNA (□), protein (△), and PG syntheses (●) is shown.

E. coli or other enterobacteria were not inhibited by lantibiotics. However, *Moraxella catarrhalis* was sensitive to them. Consistent with the mode of action of cell wall inhibitors, no activity for planosporicin was observed against *S. aureus* L-form (L3751) and the eukaryote *Candida albicans*. Because of its action on membrane permeability, nisin was indeed quite active against L-form cells.

Efficacy in Animal Models. Antibiotic planosporicin was tested in murine septicemia caused by *S. pyogenes* C203 (MIC 0.5 μg/mL) and protected mice with an ED_{50} of 3.75 mg/kg (ED_{50}/MIC = 7.5). This level of protection was observed both after intravenous (iv) and subcutaneous (sc) administrations. Teicoplanin administered sc was used as a comparative drug. It was more potent *in vitro* (MIC < 0.015 μg/mL) and protected mice with an ED_{50} of 0.18 mg/kg (ED_{50}/MIC >12). No acute toxicity was observed for up to 100 mg/kg of planosporicin after iv or sc administration.

DISCUSSION

We devised a screening process to select PG synthesis inhibitors (i) produced by uncommon actinomycetes; (ii) essentially not cross-resistant with β-lactams and glycopeptides; and (iii) effective against infections caused by Gram-positive pathogens. Through this process, we found a group of lantibiotics whose characteristics fulfilled these selection criteria. Five of them were structurally different from any of the 50 previously described lantibiotics.

Nisin, the prototype of type A lantibiotics, is a 3353 Da cationic, elongated, and flexible peptide, 34 amino acids long, containing 5 intramolecular ring structures (a single Lan and 4 Melan residues), that is produced by *Lactococcus lactis* subsp. *lactis* (*11, 12, 14*). Initially, its remarkable bactericidal action was believed to predominantly involve the formation of short-lived pores in cell membranes, causing efflux of metabolites and dissipation of vital ion gradients. More recently, it has been demonstrated that nisin interacts in a highly specific manner with lipid II, the essential membrane-bound precursor for cell wall formation, which acts as a docking molecule and energetically facilitates the formation of pores (*15, 40*).

The type B lantibiotic mersacidin is a 1825 Da, globular, hydrophobic peptide, 20 residues long, produced by a bacillus strain containing 4 thioether rings formed by 3 Melan and 1 C-terminal *S*-aminovinyl-D-methylcysteine (*16*). Mersacidin binds to lipid II, but unlike nisin, it does not form pores (*35*). The complex with lipid II differs greatly from the glycopeptide−lipid II complex and does not involve the C-terminal D-alanyl-D-alanine moiety of the pentapeptide side chain of the lipid intermediate, but equally blocks access of the transglycosylase to its substrate (*19, 38*).
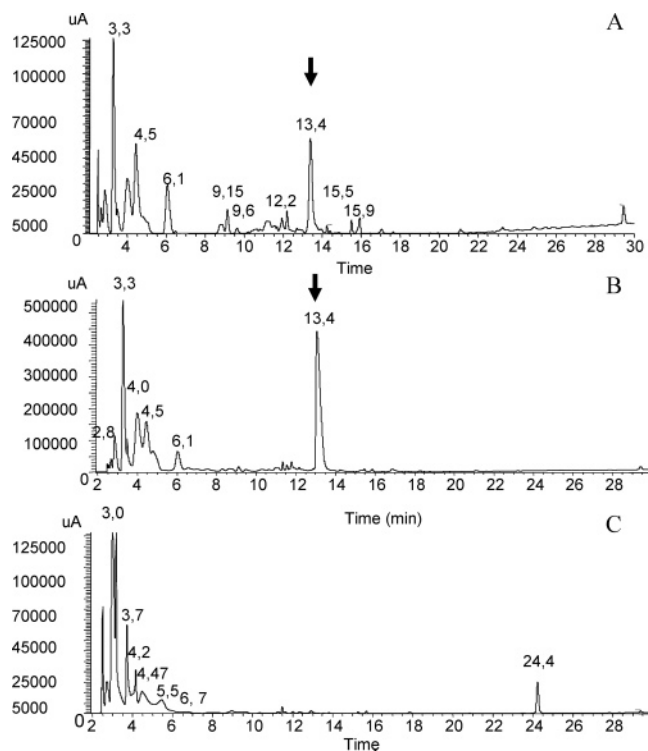
FIGURE 4: LC-MS analysis of the cell wall cytoplasmatic precursor pool in planosporicin- (A) or vancomycin-treated (B), or untreated (C) cells of *B. megaterium.* Bacterial cultures were grown, harvested, and extracted as reported in Experimental Procedures. Detection was by ESI-MS. A major peak was detectable in vancomycin- and planosporicin-treated cells at a retention time of 13.4 min (indicated by the arrow). The other peaks present on the HPLC plot showed MS profiles not related to soluble PG precursors.

Known lantibiotics of actinomycete origin all belong to the type B group and include actagardine, produced by *Actinoplanes* spp. (*17*), and cinnamycin-like peptides, produced by *Streptomyces* spp. (*14*). Actagardine is a tetracyclic 1890 Da globular peptide, 19 residues in length, which shows a significant similarity to mersacidin. Although the overall bridging pattern is quite different, one of the four rings is almost entirely conserved in both peptides, and this is likely involved in their mode of action as PG synthesis inhibitors (*12*−*14*). Lantibiotics of the cinnamycin subgroup have been reisolated several times under different names (cinnamycin, duramycin, duramycin B and C, and ancovenin), and their ring structures and amino acid compositions are very similar. Most of their bactericidal and hemolytic activity can be explained by the specific binding to phosphatidylethanolamine (*20*).

This article presents the novel antibiotic planosporicin, which is produced by the actinomycete *Planomonospora* sp. It is worthy of note that only four species belonging to the *Planomonopora* genus have been described to date, and not even one has been reported to produce any lantibiotics (*41*, *42*). The structure of planosporicin is substantially different from that of any other lantibiotic described. It is a 2194 Da polypeptide originating from 24 proteinogenic amino acids and containing 5 thioether intramolecular bridges (a single Melan and 4 Lan residues) that are predictive of conformational constraints. Indeed, NMR studies showed that the structure comprises a globular domain created by the formation of a thioether bond between residues Ala3-Ala11 and Ala7-Ala18, whereas the NH2- and COOH-terminal ends

consist of only two amino acid residues. This structure indicates that the molecule is rigid and compact because of these two large bridges (a nine-member ring Ala3- Ala11 and a twelve-member ring Ala7- Ala18) and the presence of three smaller internal loops between residues Abu8-Ala9, Ala16-Ala21, and Ala19-Ala22. In this rigid structure, a certain degree of conformational flexibility was observed in the ring formed by the 12 residues Ala7-Ala18, where three sequential glycines are located that show averaged J(NH− CHα) coupling constants of about 6 Hz. These data are consistent with the globular structure typical of type B lantibiotics.

Considering its mode of action, planosporicin is a novel member of the mersacidin-actagardine subgroup of type B lantibiotics. In whole cell experiments in *S. aureus*, planosporicin primarily inhibited PG synthesis, similarly to other cell wall inhibitors, such as actagardine and teicoplanin, but differently from nisin, which immediately blocked all of the principal macromolecular syntheses as a result of the rapid cell membrane depolarization. Planosporicin also caused accumulation of the UDP-pentapeptide precursor of PG in growing bacterial cells. Such an accumulation indicates that the multistep assembly of PG located at the membrane is inhibited; this has been observed in a series of antibiotics acting on this phase, including mersacidin and actagardine (*19*, *38*). Similar to mersacidin and actagardine, planosporicin did not bind to D-ala-D-ala peptides and showed activity against vancomycin-resistant enterococci. Despite these functional similarities, planosporicin does not contain any conserved motif resembling mersacidin and actagardine. Indeed, the initial NH2 sequence of three amino acids (NH2-Ile-Dhb-Ala) is identical to that of nisin. This sequence was found to be crucial for nisin binding to the lipid II pyrophosphate region (*44*), as demonstrated by specific mutations drastically reducing antimicrobial activities (*12*, *43*). It would be interesting to investigate whether it has the same function in planosporicin.

The *in vitro* spectrum of activity of planosporicin covered Gram-positive pathogens, including MRSA and vancomycin enterococci, which are of increasing medical importance because of the spread of resistance mechanisms. Planosporicin antimicrobial activity against Gram-positive pathogens was better than that of actagardine and comparable to that of mersacidin. Lower MICs of nisin may be explained by its dual mechanism of action, combining the sequestering of lipid II and pore formation (*15*, *40*). However, nisin is generally used as a food preservative but not in systemic chemotherapy because of its poor solubility at physiological pH, limiting its distribution in the body to the oral−gastrointestinal tract (*11*, *13*). Planosporicin was stable and soluble at physiological pH. Indeed, in a mouse experimental infection model induced by *S. pyogenes*, planosporicin showed good efficacy after a single administration. ED50-values were identical after intravenous and subcutaneous administration. This may indicate that distribution and bioavailability are comparable via the two administration routes. Good *in vivo* activity was also previously observed for mersacidin (*16*, *19*, *38*) and for actagardine (*45*), with efficacy results that exceeded expectations on the basis of the potency observed *in vitro* (*12*, *13*).

Another argument, in addition to the novelty of the binding target, supporting the chemotherapeutic exploitation of
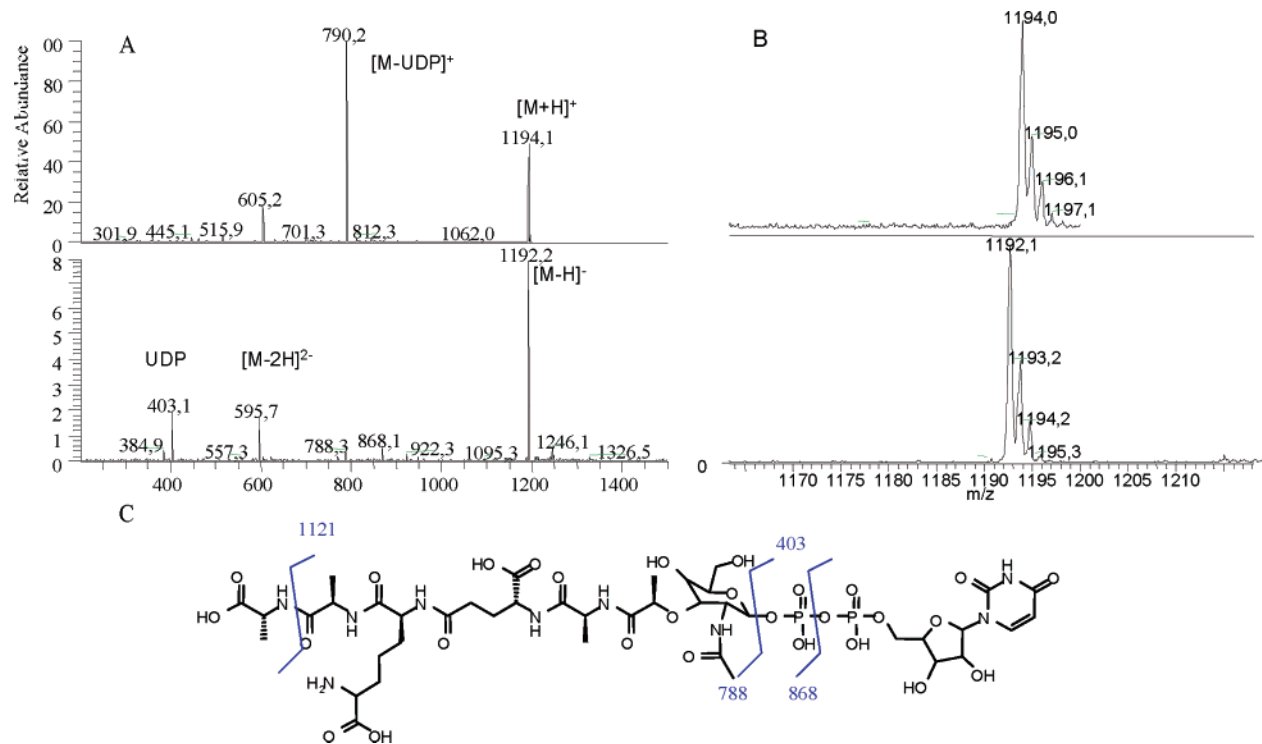
FIGURE 5: (A) Full-scan mass spectrum in negative and positive mode of the peak eluted at 13.4 min. Molecular ions [M − H]⁺ at *m/z* 1194.2 and at [M − H]⁻ at *m/z* 1192.1 correspond to the UDP-MurNAc-L-Ala-D-Glu-*m*Dap-D-Ala-D-Ala, double charged [M − H]²⁻ at *m/z* 595.7. The ion at *m/z* 403.1 corresponds to UDP formed directly in the MS source. (B) Zoom scan of the quasi-molecular ions in positive and negative ion mode. (C) Chemical structure of the UDP-MurNAc-L-Ala-D-Glu-*m*Dap-D-Ala-D-Ala and structural assignments for the main fragment ions.

Table 4: Anti-microbial Activity of Planosporicin in Comparison to that of Actagardine, Mersacidin, and Nisin[a]

strain	planosporicin	actagardine	mersacidin	nisin
L100 *Staphylococcus aureus* ATCC6538P	2	32	n.d.	0.5
L3751 *Staphylococcus aureus* L FORM	1024	>128	n.d.	16
L819 *Staphylococcus aureus* Smith ATCC19636	16	32	4	2
L1400 *Staphylococcus aureus* MRSA	16	16	8	2
L1526 *Staphylococcus aureus* MRSA	16	16	8	2
L1551 *Staphylococcus aureus* MRSA	8	16	64	8
L1577 *Staphylococcus epidermidis*	32	128	16	2
L1729 *Staph. hemeolyticus* met-r	>128	>128	8	4
L49 *Streptococcus pyogenes*	0.5	2	n.d.	n.d.
L44 *Streptococcus pneumoniae*	4	32	4	0.25
L559 *Enterococcus faecalis*	16	32	32	4
L560 *Enterococcus faecalis* Van A	64	128	64	4
L1830 *Enterococcus faecalis* Van B	32	64	64	2
L568 *Enterococcus faecium*	64	64	64	2
L569 *Enterococcus faecium* Van A	128	128	64	2
L1833 *Enterococcus faecium* Van B	16	64	64	2
L19 *Lactobacillus plantarum* ATCC08014	64	n.d.	n.d.	n.d.
L133 *Lactobacillus rhamnosus* ATCC07469	0.5	n.d.	n.d.	n.d.
L148 *Lactobacillus delbrueckii* ATCC04797	16	>128	>128	>128
L229 *Lactobacillus fermentum* ATCC09338	0.5	n.d.	n.d.	n.d.
L102 *Bacillus subtilis* ATCC6633	8	32	n.d.	n.d.
L2622 *Bacillus megaterium* ATCC13632	2	n.d.	n.d.	n.d.
L3607 *Clostridium perfringens* ATCC13124	≤0.25	4	8	≤0.13
L76 *Moraxella catarrhalis* ATCC8176	1	32	n.d.	1
L47 *Escherichia coli*	>128	>128	n.d.	>128
L145 *Candida albicans*	>128	>128	n.d.	>128

[a] MICs were determined by broth microdilution assay (*24*) according to the procedure described in Experimental Procedures (n.d., not detected).

lantibiotics is the lack of any substantial development of bacterial resistance following the extensive use of nisin in food. Lipid II is a complex target that cannot be easily altered by pathogens to acquire resistance. For instance, eight successive enzymes are required for the biosynthesis of lipid II from UDP-GlcNAc (*3*). Nevertheless, resistance can develop when bacteria are subjected to the selection pressure following repeated exposure to an antibiotic, as has been

demonstrated in vancomycin resistance when bacteria change the D-Ala-D-Ala unit of lipid II to D-Ala-D-lactate (*1, 2, 5*).

In conclusion, taking into account the structural peculiarities, the mode of action, the spectrum of activity, and the efficacy in *vivo*, planosporicin appears to be a potential new agent for the treatment of emerging resistant pathogens. Its discovery and characterization provides additional insight into the molecular determinants of the biological activity of lipid II-targeting antibiotics.

SUPPORTING INFORMATION AVAILABLE

2D NOESY spectrum (amide expanded region) of planosporicin in a mixture of H_2O/D_2O (in ratio 9:1 v/v); Table A, NOE connectivity matrix for planosporicin in H_2O/D_2O at 313 K; and Table B, ^{13}C Chemical shift (ppm) for antibiotic planosporicin in H_2O/D_2O at 313 K. This material is available free of charge via the Internet at http://pubs.acs.org.

REFERENCES

1. Appelbaum, P. C., and Jacobs, M. R. (2005) Recently approved and investigational antibiotics for treatment of severe infections caused by Gram-positive bacteria, *Curr. Opin. Microbiol. 8*, 510–517.
2. Appelbaum, P. C. (2006) The emergence of vancomycin-intermediate and vancomycin-resistant *Staphylococcus aureus*, *Clin. Microbiol. Infect. 12*, 16–23.
3. Walsh, C. (2003) Antibiotics that Block Cell Wall Biosynthesis, in *Antibiotics. Actions, Origins, Resistance*, pp 23–49, ASM Press, Washington, D.C.
4. Birnbaum, J., Kahan, F. M., Kropp, H., MacDonald, J. S., Kahan, J. S., Goegelman, R., Currie, S. A., Jackson, M., Stapley, E. O., Miller, T. W., Miller, A. K., Hendlin, D., Mochales, S., Hernandez, S., and Woodruff, H. B. (1985) Carbapenems, a new class of beta-lactam antibiotics. Discovery and development of imipenem/cilastatin, *Am. J. Med. 78*, 3–21.
5. Johnson, A. P., Uttley, A. H., Woodford, N., and George, R. C. (1990) Resistance to vancomycin and teicoplanin: an emerging clinical problem, *Clin. Microbiol. Rev. 3*, 280–291.
6. Parenti, F., Beretta, G., Berti, M., and Arioli, V. (1978) Teichomycins, new antibiotics from *Actinoplanes teichomyceticus* Nov. Sp. I. Description of the producer strain, fermentation studies and biological properties, *J. Antibiot. 31*, 276–283.
7. Goldstein, B. P., Selva, E., Gastaldo, L., Berti, M., Pallanza, R., Ripamonti, F., Ferrari, P., Denaro, M., Arioli, V., and Cassani, G. (1987) A40926, a new glycopeptide antibiotic with anti-*Neisseria* activity, *Antimicrob. Agents Chemother. 31*, 1961–1966.
8. Malabarba, A., and Goldstein, B. P. (2005) Origin, structure, and activity *in vitro* and *in vivo* of dalbavancin, *J. Antimicrob. Chemother. 55* 15–20.
9. Parenti, F., Ciabatti, R., Cavalleri, B., and Kettenring, J. (1990) Ramoplanin: a review of its discovery and its chemistry, *Drugs Exp. Clin. Res .16*, 451–455.
10. Lazzarini, A., Cavaletti, L., Toppo, G., and Marinelli, F. (2001) Rare genera of actinomycetes as potential producers of new antibiotics, *Antonie van Leeuwenhoek 79*, 399–405.
11. Jung, G. (1991) Lantibiotics- A Survey, in *Nisin and Novel Lantibiotics* (Jung, G., and Sahl, H. G., Eds.) pp 1–34, ESCOM, Leiden, The Netherlands.
12. Chatterjee, C., Paul, M., Xie, L., and van der Donk, W. A. (2005) Biosynthesis and mode of action of lantibiotics, *Chem. Rev. 105*, 633–684.
13. Cotter, P. D., Hill, C., and Ross, R. P. (2005) Bacterial lantibiotics: strategies to improve therapeutic potential, *Curr. Protein Pept. Sci. 6*, 61–75.
14. Pag, U., and Sahl, H. G. (2002) Multiple activities in lantibiotics–models for the design of novel antibiotics? *Curr. Pharm. Des. 8*, 815–833.
15. Breukink, E., Wiedemann, I., van Kraaij, C., Kuipers, O. P., Sahl, H., and de Kruijff, B. (1999) Use of the cell wall precursor lipid II by a pore-forming peptide antibiotic, *Science 286*, 2361–2364.
16. Chatterjee, S., Chatterjee, D. K., Jani, R. H., Blumbach, J., Ganguli, B. N., Klesel, N., Limbert, M., and Seibert, G. (1992) Mersacidin, a new antibiotic from *Bacillus. In vitro* and *in vivo* antibacterial activity, *J. Antibiot. 45*, 839–845.
17. Somma, S., Merati, W., and Parenti, F. (1977) Gardimycin, a new antibiotic inhibiting peptidoglycan synthesis, *Antimicrob. Agents Chemother. 11*, 396–401.
18. Parenti, F., Pagani, H., and Beretta, G. (1976) Gardimycin, a new antibiotic from *Actinoplanes*. I. Description of the producer strain and fermentation studies, *J. Antibiot. 29*, 501–506.
19. Brotz, H., Bierbaum, G., Leopold, K., Reynolds, P. E., and Sahl, H. G. (1998) The lantibiotic mersacidin inhibits peptidoglycan synthesis by targeting lipid II, *Antimicrob. Agents Chemother. 42*, 154–160.
20. Machaidze, G., and Seelig, J. (2003) Specific binding of cinnamycin (Ro 09-0198) to phosphatidylethanolamine. Comparison between micellar and membrane environments, *Biochemistry 42*, 12570–12576.
21. Hatano, K., and Nishino, T. (1994) Morphological alterations of *Staphylococcus aureus* and *Streptococcus pyogenes* exposed to cefdinir, a new oral broad-spectrum cephalosporin, *Chemotherapy 40*, 73–79.
22. Losi, D., Cavaletti, L., Lazzarini, A., Candiani, G., Castiglione, F., and Marinelli, F. (2004) Antibiotics ID 97518, Pharmaceutically Acceptable Salts and Compositions, and Use Thereof, Eur. Pat. 1481986A1, Dec 1.
23. Jass, J., Phillips, L. E., Allan, E. J., Costerton, J. W., and Lappin-Scott, H. M. (1994) Growth and adhesion of *Enterococcus faecium* L-forms, *FEMS Microbiol. Lett. 115*, 157–162.
24. NCCLS (1990) *Approved Standard M7–A2. Methods for Dilution Antimicrobial Susceptibility Testing for Bacteria that Grow Anaerobically*, 2nd ed., Villanova University: Villanova, PA.
25. Corti, A., Rurali, C., Borghi, A., and Cassani, G. (1985) Solid-phase enzyme-receptor assay (SPERA): a competitive-binding assay for glycopeptide antibiotics of the vancomycin class, *Clin. Chem. 31*, 1606–1610.
26. Kohlrausch, U., and Holtje, J. V. (1991) One-step purification procedure for UDP-N-acetylmuramyl-peptide murein precursors from *Bacillus cereus, FEMS Microbiol. Lett. 62*, 253–257.
27. Finney, D. J. (1952) The Spearman-Kärber Method, in *Statistical Methods in Biological Assay*, pp 524–530, Charles Griffin & Co., Ltd., London, England.
28. Meiring, H. D., Van der Heeft, E., Ten Hove, G. J., and de Jong, A. P. J. (2002) Nanoscale LC-MS(n): Technical design and applications to peptide and protein analysis, *J. Sep. Sci. 25*, 557–568.
29. Pawlowska, M., Chen, S., and Armstrong, D. W. (1993) Enantiomeric separation of fluorescent, 6-aminoquinolyl-N-hydroxysuccinimidyl carbamate, tagged amino acids, *J. Chromatogr. 641*, 257–265.
30. Bax, A., and Devis, D. G. (1985) MLEV-17-based two-dimensional homonuclear magnetization transfer spectroscopy, *J. Magn. Reson. 65*, 355–360.
31. Griesinger, C., Otting, G., Wuethrich, K., and Ernst, R. R. (1988) Clean TOCSY for 1H spin system identification in macromolecules, *J. Am. Chem. Soc. 110*, 7870–7872.
32. Wishart, D. S., and Nip, A. M. (1998) Protein chemical shift analysis: a practical guide, *Biochem. Cell Biol. 76*, 153–163.
33. Wuthrich, K. (1986) *NMR of Proteins and Nucleic Acids*, Wiley, New York.
34. Cierpicki, T., and Otlewski, J. (2001) Amide proton temperature coefficients as hydrogen bond indicators in proteins, *J. Biomol. NMR 21*, 249–261.
35. Hsu, S. T., Breukink, E., Bierbaum, G., Sahl, H. G., de Kruijff, B., Kaptein, R., van Nuland, N. A., and Bonvin, A. M. (2003) NMR study of mersacidin and lipid II interaction in dodecylphosphocholine micelles. Conformational changes are a key to antimicrobial activity, *J. Biol. Chem. 278*, 13110–13117.
36. Billot-Klein, D., Shlaes, D., Bryant, D., Bell, D., Legrand, R., Gutmann, L., and van Heijenoort, J. (1997) Presence of UDP-N-acetylmuramyl-hexapeptides and -heptapeptides in enterococci and staphylococci after treatment with ramoplanin, tunicamycin, or vancomycin, *J. Bacteriol. 179*, 4684–4688.
37. Ruzin, A., Singh, G., Severin, A., Yang, Y., Dushin, R. G., Sutherland, A. G., Minnick, A., Greenstein, M., May, M. K., Shlaes, D. M., and Bradford, P. A. (2004) Mechanism of action of the mannopeptimycins, a novel class of glycopeptide antibiotics active against vancomycin-resistant gram-positive bacteria, *Antimicrob. Agents Chemother. 48*, 728–738.

38. Brotz, H., Bierbaum, G., Reynolds, P. E., and Sahl, H. G. (1997) The lantibiotic mersacidin inhibits peptidoglycan biosynthesis at the level of transglycosylation, *Eur. J. Biochem. 246*, 193−199.

39. Cannon, J. P., Lee, T. A., Bolanos, J. T., and Danziger, L. H. (2005) Pathogenic relevance of *Lactobacillus*: a retrospective review of over 200 cases, *Eur. J. Clin. Microbiol. Infect. Dis. 24*, 31−40.

40. Hasper, H. E., Kramer, N. E., Smith, J. L., Hillman, J. D., Zachariah, C., Kuipers, O. P., de Kruijff, B., and Breukink, E. (2006) An alternative bactericidal mechanism of action for lantibiotic peptides that target lipid II, *Science 313*, 1636−1637.

41. Mertz, F. P. (1994) *Planomonospora alba* sp. nov. and *Planomonospora sphaerica* sp. nov., two new species isolated from soil by baiting techniques, *Int. J. Syst. Bacteriol. 44*, 274−281.

42. Vobis, G. (1989) Genus *Planomonospora*, in *Bergey's Manual of Systematic Bacteriology* (Wilkins, W. A., Ed.) pp 2539−2543, Baltimore, MD.

43. Wiedemann, I., Breukink, E., van Kraaij, C., Kuipers, O. P., Bierbaum, G., de Kruijff, B., and Sahl, H. G. (2001) Specific binding of nisin to the peptidoglycan precursor lipid II combines pore formation and inhibition of cell wall biosynthesis for potent antibiotic activity, *J. Biol. Chem. 276*, 1772−1779.

44. Hsu, S. T., Breukink, E., Tischenko, E., Lutters, M. A., de Kruijff, B., Kaptein, R., Bonvin, A. M., and van Nuland, N. A. (2004) The nisin-lipid II complex reveals a pyrophosphate cage that provides a blueprint for novel antibiotics, *Nat. Struct. Mol. Biol. 11*, 963−967.

45. Arioli, V., Berti, M., and Silvestri, L. G. (1976) Gardimycin, a new antibiotic from *Actinoplanes*. III. Biological properties, *J. Antibiot. 29*, 511−515.